

# Microscopic Reaction Dynamics at SPS and RHIC

Steffen A. Bass<sup>a</sup>

<sup>a</sup>Department of Physics, Duke University, Durham, NC 27708-0305

RIKEN-BNL Research Center, Brookhaven National Laboratory, Upton, NY11973

## 1. Transport Theory at RHIC

Transport Theory offers the unique capability of connecting experimentally observable quantities in a relativistic heavy ion collision with its time evolution and reaction dynamics, thus giving crucial insights into the possible formation of a transient deconfined phase of hot and dense matter, the Quark-Gluon-Plasma (for reviews on QGP signatures, see e.g. [1,2]).

Figure 1 provides an overview of different transport theoretical ansatzes currently on the market for the description of a relativistic heavy ion collision at RHIC energies. The timeline shows a *best case scenario* for what to expect: the formation of a QGP with subsequent hadronization and freeze-out. Bands with solid lines denote the safe range of applicability for the respective transport approach, whereas dashed/dotted bands refer to areas in which the approach is still applied but where the assumptions on which the approach is based upon may be questionable or not valid anymore.

The *initial state* and early *pre-equilibrium phase* are best described in Classical Yang-Mills theory (CYM) [3] or Lattice Gauge Transport (LGT) [4] calculations - only these classes of models treat the coherence of the initial state correctly, but do not provide any meaningful dynamics for the later reaction stages.

The Parton Cascade Model (PCM) [5] and related pQCD approaches [6] treat the initial state as incoherent parton configuration, but are very well suited for the *pre-equilibrium phase* and subsequent thermalization, leading to a *QGP and hydrodynamic expansion*. Microscopic degrees of freedom in this ansatz are quarks and gluons which are propagated according to a Boltzmann Equation with a collision term using leading order pQCD cross sections. Augmented with a cluster hadronization ansatz the PCM is applicable up to *hadronization*. The range of this model can be even further extended if it is combined with a hadronic cascade which treats the *hadronic phase and freeze-out* correctly [7].

Nuclear Fluid Dynamics (NFD, see e.g. [8,9]) is ideally suited for the *QGP and hydrodynamic expansion* reaction phase, but breaks down in the later, dilute, stages of the reaction when the mean free paths of the hadrons become large and flavor degrees of freedom are important. The reach of NFD can also be extended by combining it with a microscopic hadronic cascade model – this kind of hybrid approach (dubbed *hydro plus micro*) was pioneered in [10] and has been now also taken up by other groups [11]. It is to date the most successful approach for describing the soft physics at RHIC. The biggest

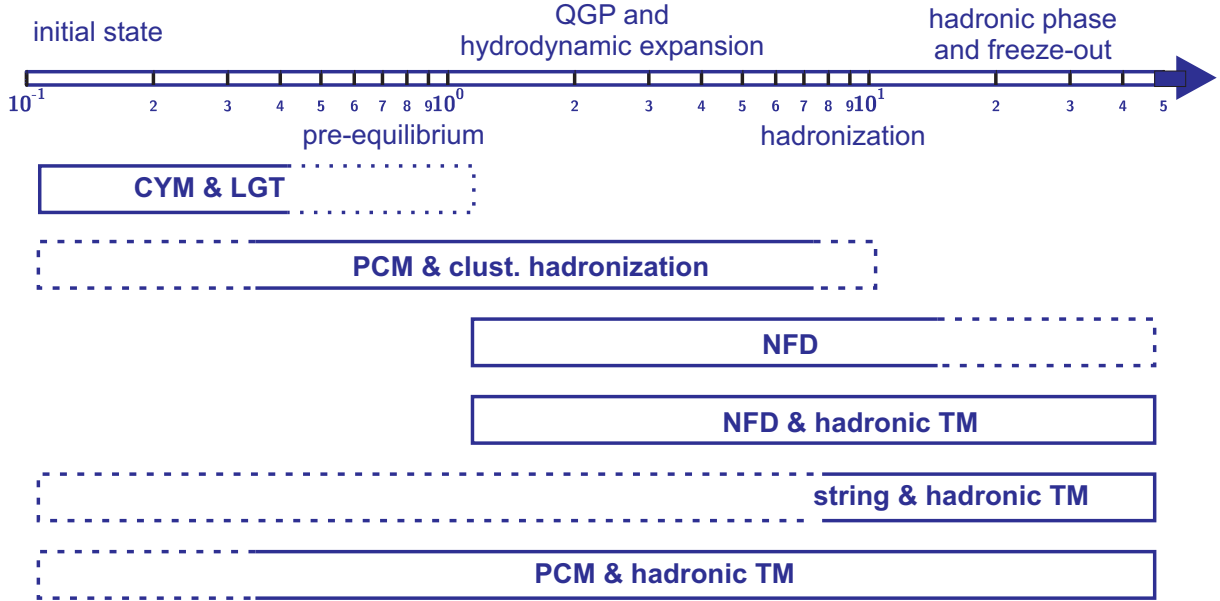


Figure 1. Transport theory approaches for RHIC and their range of applicability.

advantage of NFD is that it directly incorporates an equation of state as input - one of its largest disadvantages is that it requires thermalized initial conditions and one is not able to do an ab-initio calculation.

Last but not least string and hadronic transport models [12,13] have been very successful in the AGS and SPS energy domains. They treat the early reaction phase as a superposition of hadron-hadron strings and are thus ill suited to describe the microscopic reaction dynamics of deconfined degrees of freedom. In the later reaction stages, however, they are the best suited approach, since they incorporate the full spectrum of degrees of freedom of a hadron gas (including flavor dependent cross sections).

It is thus important to note that there is not a single transport theoretical ansatz currently available, which is able to cover the entire time-evolution of a collision at RHIC in one self-consistent approach.

## 2. Kinetic Evolution

The initial reaction dynamics are best described by partonic degrees of freedom. Figure 2 shows the time-evolution of the average squared momentum transfer  $\langle Q^2 \rangle$  in parton-parton collisions for central Au+Au reactions at RHIC, based on a PCM calculation [14]. Early rescatterings of incident partons occur at rather large values of  $Q^2 \approx 7 \text{ GeV}^2$ . However, between the time  $t_{\text{c.m.}} \approx 0.5 \text{ fm}/c$  and  $t_{\text{c.m.}} \approx 4.5 \text{ fm}/c$  the average  $\langle Q^2 \rangle$  decreases rapidly to a value of about  $4.5 \text{ GeV}^2$  until hadronization sets in. The strong time-dependence of  $\langle Q^2 \rangle$  shows that there is no single  $Q^2$  scale which can be chosen to unambiguously set the pQCD scale in an ultra-relativistic heavy-ion collision. The reaction dynamics in the partonic phase is dominated by gluon-gluon scattering ( $\approx 43\%$ ) followed gluon fusion ( $\approx 27\%$ ) and quark-gluon scattering ( $\approx 26\%$ ). Quark-quark and quark-antiquark scattering only contribute on a few % level. These numbers are fairly

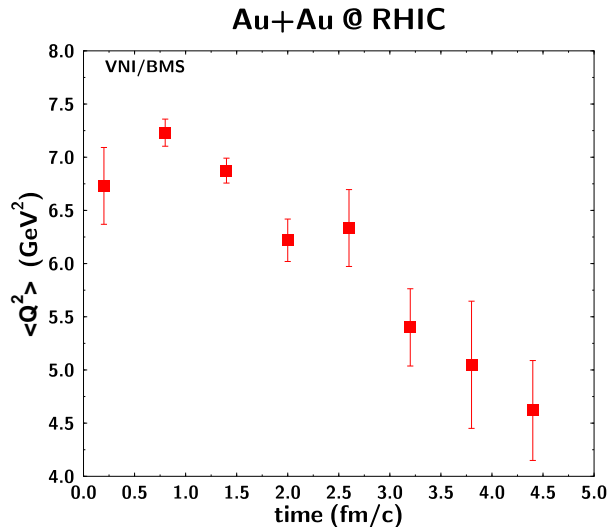


Figure 2. Time evolution of parton scattering  $\langle Q^2 \rangle$  for central Au+Au collisions at RHIC in the Parton Cascade Model

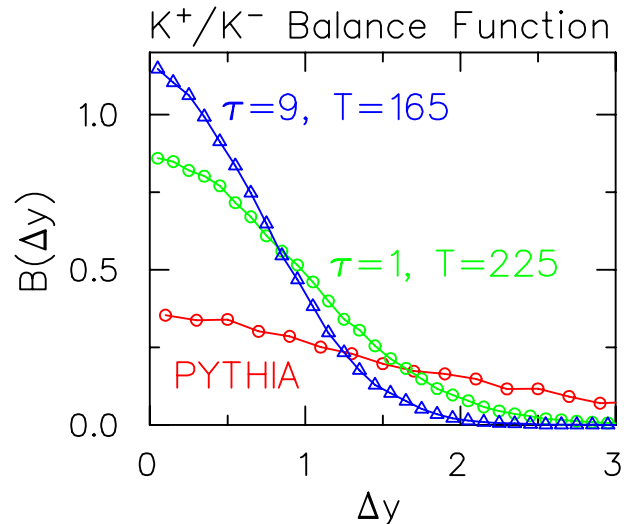


Figure 3.  $K^+/K^-$  Balance Functions for  $T_C = 165$  MeV,  $T_C = 225$  MeV and in a hadronizing string picture

independent of the system size and change only marginally between proton-proton and Au+Au reactions.

While there is no doubt about the importance of partonic degrees of freedom for the initial, early, reaction stages, the crucial question is, how long the deconfined state actually existed and whether this time-span is long enough for thermalization and collective effects to occur. Balance functions offer a unique model-independent formalism to probe the time-scales of a deconfined phase and subsequent hadronization [15]. Late-stage production of quarks could be attributed to three mechanisms: formation of hadrons from gluons, conversion of the non-perturbative vacuum energy into particles, or hadronization of a quark gas at constant temperature. Hadronization of a quark gas should approximately conserve the net number of particles due to the constraint of entropy conservation. Since hadrons are formed of two or more quarks, creation of quark-antiquark pairs should accompany hadronization. All three mechanisms for late-stage quark production involve a change in the degrees of freedom. Therefore, any signal that pinpoints the time where quarks first appear in a collision would provide valuable insight into understanding whether a novel state of matter has been formed and persisted for a substantial time.

The link between balance functions and the time at which quarks are created has a simple physical explanation. Charge-anticharge pairs are created at the same location in space-time, and are correlated in rapidity due to the strong collective expansion inherent to a relativistic heavy ion collision. Pairs created earlier can separate further in rapidity due to the higher initial temperature and due to the diffusive interactions with other particles. The balance function, which describes the momentum of the accompanying antiparticle, quantifies this correlation. The balance function describes the conditional probability that a particle in the bin  $p_1$  will be accompanied by a particle of opposite charge in the bin  $p_2$ :

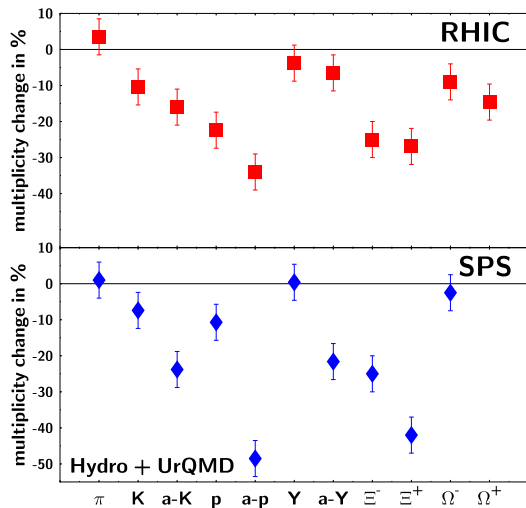


Figure 4. Multiplicity change in % due to hadronic rescattering for various hadron species at SPS and RHIC. The error-bars give an estimate of the systematic error.

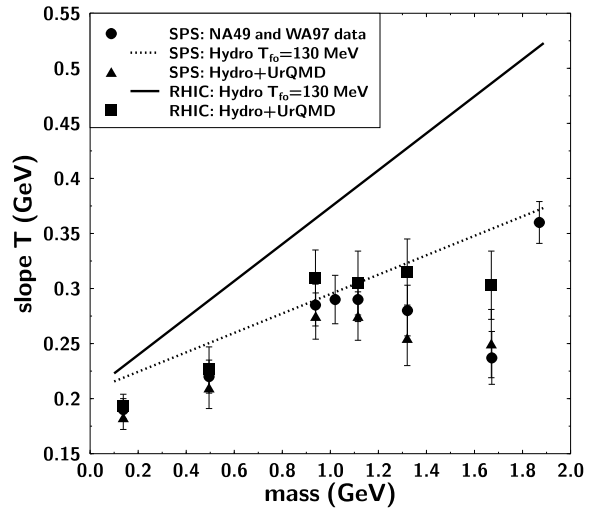


Figure 5. Inverse hadron  $m_T$  slopes at  $y_{c.m.} = 0$ . The lines depict pure hydrodynamics whereas the symbols refer to data and hydro+micro calculations.

$$B(p_2|p_1) \equiv \frac{1}{2} \{ \rho(b, p_2|a, p_1) - \rho(b, p_2|b, p_1) + \rho(a, p_2|b, p_1) - \rho(a, p_2|a, p_1) \}, \quad (1)$$

where  $\rho(b, p_2|a, p_1)$  is the conditional probability of observing a particle of type  $b$  in bin  $p_2$  given the existence of a particle of type  $a$  in bin  $p_1$ . The label  $a$  might refer to all negative kaons with  $b$  referring to all positive kaons, or  $a$  might refer to all hadrons with a strange quark while  $b$  refers to all hadrons with an antistrange quark.

Figure 3 shows  $K^+/K^-$  balance functions as predicted in a simple Bjorken thermal model for two hadronization temperatures, 225 MeV and 165 MeV as well as for fragmenting strings (utilizing PYTHIA), which would represent the hadronization scenario of a hadronic/string picture similar to that of RQMD or UrQMD. Since particles from cooler systems have smaller thermal velocities, they are more strongly correlated in rapidity and result in narrower balance functions. A strong sensitivity to the hadronization temperature and time can be clearly observed.

### 3. Flavor Evolution

A central issue for the characterization of the deconfined phase on the basis of the measurable final state hadrons is how much the hadronic composition of the system changes due to hadronic rescattering: figure 4 shows the relative change (in %) of the multiplicity for various hadron species at SPS and RHIC between hadronization and freeze-out. As is to be expected, the state of rapid expansion prevailing at hadronization does not allow chemical equilibrium to hold down to much lower temperatures. The hadronic rescattering changes the multiplicities by less than a factor of two, cf. also [16]. Thus, we have first evidence that a QGP expanding and hadronizing as an ideal fluid produces a too rapidly expanding background for a hadron-fluid with known elementary cross-sections to maintain chemical equilibrium down to much lower temperatures than  $T_C$ .

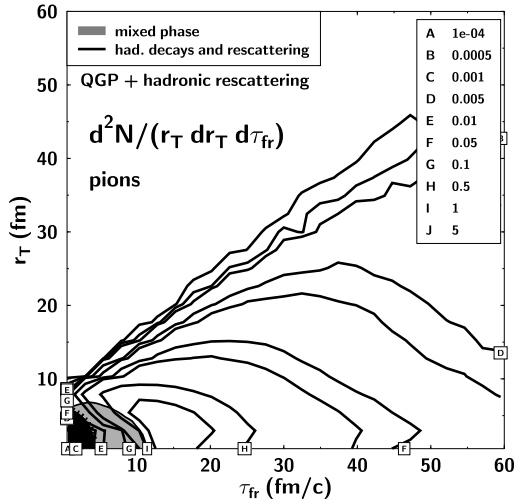


Figure 6. Freeze-out transverse radius and time distribution  $d^2 N / (r_T dr_T dt_{fr})$  for pions at RHIC.

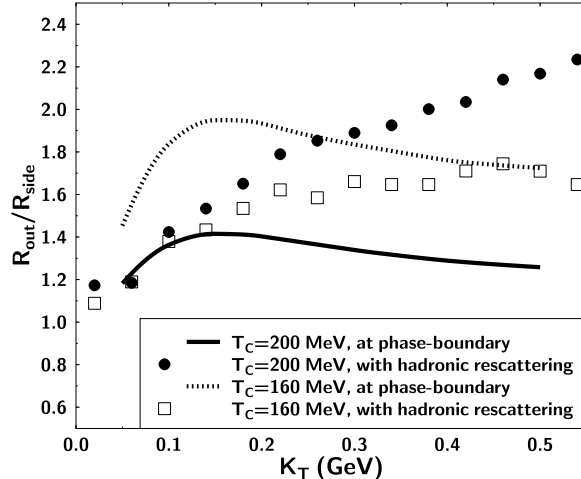


Figure 7.  $R_{out}/R_{side}$  for RHIC initial conditions, as a function of  $K_T$  at freeze-out (symbols) and at hadronization (lines).

However, a closer look provides more insight into the chemical composition. The changes are most pronounced at the SPS, where the baryon-antibaryon asymmetry is highest (since the net-baryon density at mid-rapidity is highest). This manifests e.g. in a reduction of the antiproton multiplicity by 40-50% due to baryon-antibaryon annihilation.  $\bar{\Lambda}$  and  $\bar{\Xi}$  are affected in similar fashion. It remains a matter of debate whether these changes in the hadronic yields are consistent with the assumption of chemical freeze-out at the phase-boundary.

However, despite the large amount of rescattering occurring in the hadronic phase, some hadron species may yet be sensitive to conditions at hadronization: figure 5 displays the inverse slope parameters  $T$  obtained by an exponential fit to  $dN_i/d^2m_T dy$  in the range  $m_T - m_i < 1$  GeV for SPS and RHIC in a hybrid hydro+micro calculation and compares them to SPS data [17]. The trend of the data, namely the “softer” spectra of  $\Xi$ 's and  $\Omega$ 's as compared to a linear  $T(m)$  relation is reproduced reasonably well. This is in contrast to “pure” hydrodynamics with kinetic freeze-out on a common hypersurface (e.g. the  $T = 130$  MeV isotherm), where the stiffness of the spectra increases linearly with mass as denoted by the lines in fig. 5. When going from SPS to RHIC energy, the model discussed here generally yields only a slight increase of the inverse slopes, although the specific entropy is larger by a factor of 4-5! The reason for this behavior is the first-order phase transition that softens the transverse expansion considerably.

The softening of the spectra is caused by the hadron gas emerging from the hadronization of the QGP being almost “transparent” for the multiple strange baryons. This can be seen by calculating the average number of collisions different hadron species suffer in the hadronic phase: whereas  $\Omega$ 's suffer on average only one hadronic interaction,  $N$ 's and  $\Lambda$ 's suffer approx. 5–6 collisions with other hadrons before they freeze-out.

Thus, one may conclude that the spectra of  $\Xi$ 's and especially  $\Omega$ 's are practically unaffected by the hadronic reaction stage and closely resemble those on the phase boundary.

They therefore act as probes of the QGP expansion prior to hadronization and can be used to measure the expansion rate of the deconfined phase.

#### 4. Freeze-out

Kinetic freeze-out, at which all (elastic) interactions cease, terminates the evolution of the reaction discussed in figure 1. However, the freeze-out time of the system is ill-defined, since interactions cease locally on a particle per particle basis. Fig. 6 shows the distribution of freeze-out points of pions in the forward light-cone, as well as the hadronization hypersurface from where all hadrons emerge in a hydro+micro approach. Freeze-out is seen to occur in a *four-dimensional* region within the forward light-cone rather than on a three-dimensional “hypersurface” in space-time. Similar results have also been obtained within other microscopic transport models [18] when the initial state was not a QGP. It is clear that the hadronic system disintegrates slowly (as compared to e.g. the hadronization time), rather than emitting a “flash” of hadrons (predominantly pions) in an instantaneous decay.

A first order phase transition leads to a prolonged hadronization time as compared to a cross-over or ideal hadron gas with no phase transition, and has been related to unusually large Hanbury-Brown–Twiss (HBT) radii [19–21]. The phase of coexisting hadrons and QGP reduces the “explosivity” of the high-density matter before hadronization, extending the emission duration of pions [19–21]. This phenomenon should then depend on the hadronization (critical) temperature  $T_c$  and the latent heat of the transition. For recent reviews on this topic we refer to [22,23].

It has been suggested that the ratio  $R_{\text{out}}/R_{\text{side}}$  should increase strongly once the initial entropy density  $s_i$  becomes substantially larger than that of the hadronic gas at  $T_c$  [21]. The strong  $T_c$  dependence of  $R_{\text{out}}/R_{\text{side}}$  in such a purely hydrodynamical scenario can be seen in fig. 7 (solid and dotted lines). Here, the  $R_{\text{out}}/R_{\text{side}}$  ratio at hadronization (calculated in a hydrodynamical scenario) is compared to the ratio after subsequent hadronic rescattering and freeze-out in a combined hydro+micro approach [24]. Clearly, up to  $K_T \sim 200$  MeV  $R_{\text{out}}/R_{\text{side}}$  is independent of  $T_c$ , if hadronic rescatterings are taken into account. Moreover, at higher  $K_T$  the dependence on  $T_c$  is even reversed: for high  $T_c$  the  $R_{\text{out}}/R_{\text{side}}$  ratio even exceeds that for low  $T_c$ . Higher  $T_c$  speeds up hadronization but on the other hand prolongs the dissipative hadronic phase that dominates the HBT radii. This is because during the non-ideal hadronic expansion the scale of spatial homogeneity of the pion density distribution increases, as the pions fly away from the center, but the transverse flow can hardly increase to counteract. Therefore, after hadronic rescattering  $R_{\text{out}}/R_{\text{side}}$  does not drop towards higher  $K_T$  (in the range  $K_T \lesssim 3m_\pi$ ).

For central collisions of Au nuclei at  $\sqrt{s} = 130A$  GeV, preliminary data from STAR gives  $R_{\text{out}}/R_{\text{side}} \simeq 1.1$  at small  $K_T$  [25]. Results from RHIC at higher  $K_T$  will test whether a long-lived *hadronic* soft-rescattering stage, associated with the formation and hadronization of an equilibrated QGP state is indeed seen in heavy ion collisions at the highest presently attainable energies.

I wish to thank my collaborators A. Dumitru, P. Danielewicz, B. Müller, S. Pratt, S. Soff, D. Srivastava and the UrQMD collaboration, who have significantly contributed to the results reviewed in this article. This work was supported by DOE grant DE-FG02-

96ER40945.

## REFERENCES

1. S. A. Bass, M. Gyulassy, H. Stöcker and W. Greiner, J. Phys. **G25**, R1 (1999).
2. J. Harris and B. Müller, Ann. Rev. Nucl. Part. Sci. **46**, 71 (1996)
3. L. McLerran and R. Venugopalan, Phys. Rev. D **49**, 3352 (1994); Phys. Rev. D **49**, 2233 (1994).
4. W. Poschl and B. Muller, Phys. Rev. D **60**, 114505 (1999); S. A. Bass, B. Muller and W. Poschl, J. Phys. **GG25**, L109 (1999).
5. K. Geiger, Phys. Rept. **258**, 237 (1995).
6. X. Wang and M. Gyulassy, Phys. Rev. D **44**, 3501 (1991).
7. S. A. Bass, M. Hofmann, M. Bleicher, L. Bravina, E. Zabrodin, H. Stoecker and W. Greiner, Phys. Rev. C **60**, 021901 (1999).
8. J.D. Bjorken, Phys. Rev. **D27**, 140 (1983);  
K. Kajantie and L. McLerran, Nucl. Phys. **B214**, 261 (1983).
9. A. Dumitru and D. Rischke, Phys. Rev. **C59**, 354 (1999).
10. S. A. Bass and A. Dumitru, Phys. Rev. **C61**, 064909 (2000).
11. D. Teaney, J. Lauret and E. V. Shuryak, nucl-th/0011058.
12. H. Sorge, H. Stocker and W. Greiner, Annals Phys. **192**, 266 (1989).
13. S. A. Bass *et al.*, Prog. Part. Nucl. Phys. **41**, 225 (1998); M. Bleicher *et al.*, J. Phys. **G25**, 1859 (1999).
14. S.A. Bass, B. Müller and D.K. Srivastava, manuscript in preparation.
15. S. A. Bass, P. Danielewicz and S. Pratt, Phys. Rev. Lett. **85**, 2689 (2000).
16. R. Stock, Phys. Lett. **B456**, 277 (1999); U. Heinz, Nucl. Phys. A **661**, 140 (1999).
17. E. Andersen *et al.* (WA97 collaboration), Phys. Lett **B433** 209 (1998).  
R. Lietava *et al.* (WA97 collaboration), Journal of Physics **G25** 181 (1999).  
R. Caliendo *et al.* (WA97 collaboration), Journal of Physics **G25** 171 (1999).  
S. Margetis *et al.* (NA49 collaboration), Journal of Physics **G25** 189 (1999).  
F. Gabler *et al.* (NA49 collaboration), Journal of Physics **G25** 199 (1999).  
D. Evans *et al.* (WA85 and WA94 collaborations), Journal of Physics **G25** 209 (1999).
18. L. V. Bravina, I. N. Mishustin, N. S. Amelin, J. P. Bondorf and L. P. Csernai, Phys. Lett. **B354**, 196 (1995); H. Sorge, Phys. Lett. **B373**, 16 (1996); S. Pratt and J. Murray, Phys. Rev. C **57**, 1907 (1998).
19. S. Pratt, Phys. Rev. **D33**, 1314 (1986);
20. B. R. Schlei, U. Ornik, M. Plümer and R. M. Weiner, Phys. Lett. **B293**, 275 (1992);  
J. Bolz, U. Ornik, M. Plümer, B. R. Schlei and R. M. Weiner, Phys. Rev. **D47**, 3860 (1993).
21. D. Rischke, M. Gyulassy, Nucl. Phys. **A608**, 479 (1996).
22. R. M. Weiner, Phys. Rept. **327**, 249 (2000); T. Csörgő, hep-ph/0001233.
23. U. Wiedemann and U. Heinz, Phys. Rept. **319**, 145 (1999).
24. S. Soff, S.A. Bass and A. Dumitru, Phys. Rev. Lett. in print, [nucl-th/0012085].
25. J. Harris, F. Laue, and S. Panitkin, talks given at Quark Matter 2001, see these proceedings.